PVF_2 TRANSDUCERS FOR NDT

E. Carome, K. Fesler, H. J. Shaw, D. Weinstein, and L. T. Zitelli
Edward L. Ginzton Laboratory
Stanford University
Stanford, CA. 94305

ABSTRACT

We have investigated the spatial dependence of the longitudinal piezoelectric stress constant e_{zz} of PVF_2. Experiments were performed on a series of nominally identical brass-backed PVF_2 longitudinal wave transducers in water using commercial PVF_2 film. Computer programs were designed to predict the performance of the transducers as a function of $e_{zz}(Z)$, the thickness mode piezoelectric stress constant as a function of position Z through the thickness of the film. Our experiments indicate that the coupling coefficient is uniform across the film thickness. These computer programs were also used to model the insertion loss and bandwidth performance of the transducers. High voltage pulses were applied to PVF_2 transducers to determine the region of linearity and to find the maximum nondestructive voltage that can be used. Transducers of this type were also made using PVF_2 films fabricated in the Stanford Center for Materials Research using commercial resin, and found to perform as well as transducers using commercial film. Transducers of the above kind have also been used as bulk wave sources in wedge transducer assemblies for the production of surface acoustic waves on ceramic plates, and initial observations of reflections from surface cracks have been made.

It has been reported the PVF_2 film may have a spatially non-uniform piezoelectric coupling coefficient.[1] The claim is that the active piezoelectric region is concentrated near the positive side of the film, the positive side being the side that was charged positively during the poling process. The PVF_2 transducer, which consists of a piece of electroded PVF_2 bonded to a brass backing,[2] may have either the positive or negative side of the film exposed. The two possible configurations are shown below in Fig. 1. If the piezoelectric coupling constant is non-uniform across the thickness of the film, the insertion loss characteristics of a PVF_2 transducer should depend on the configuration of the transducer. This statement was verified using a computer matrix model that calculated the insertion loss of a single multi-layer PVF_2 transducer transmitting into water.[3]

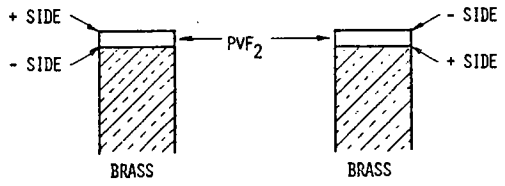

Fig. 1. Schematic of the PVF_2 brass-backed transducer configurations[2] used.

Results obtained using this program are shown in Fig. 2. The PVF_2 was modeled as ten separate 3.1 μ thick layers,[2] with e_{zz} values of (.1, .05, .025, .0125, .00625, .003125, 0, 0, 0, 0) in order across the 10 layers. The top curve is the predicted insertion loss when the layer with the maximum e_{zz} value is located next to the loading material (water). This configuration results in a resonance valley around $\omega = .6\ \omega_0$ due to the layer of nonpiezoelectric PVF_2 trapped between the backing material (brass) and the active PVF_2. The bottom curve is the predicted insertion loss when the layer with $e_{zz} = .1$ is located next to the brass.

Figure 2 shows that large insertion loss differences should be apparent if e_{zz} is strongly non-homogenous.

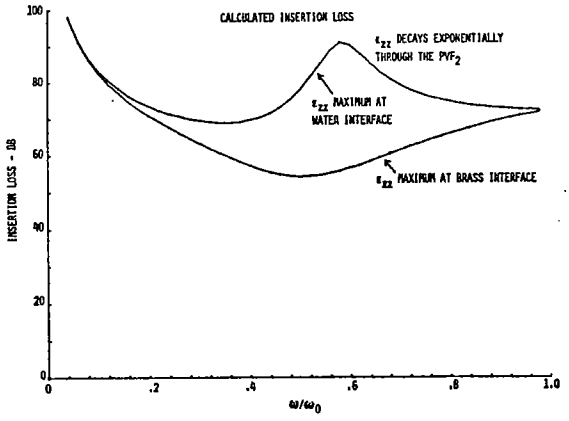

Fig. 2. Calculated insertion loss curves for PVF_2 with non-homogenous value of e_{zz}.

Six brass backed PVF_2 transducers were constructed using 25 μ thick[2] film obtained from Kureha Corp. The aluminum electrodes originally on the PVF_2 were removed and replaced by a flash of chromium and a thin layer of gold (~ 1000 Å), deposited using an e-gun evaporation system. The polymer was then repoled with a voltage of 2500 volts (≈ 10^6 V/cm) placed across the PVF_2 for two hours. The positive electrode of the poling apparatus was connected to the side of the PVF_2 which had been poled positively by Kureha. The poling was performed in an air oven, at a temperature of 80°C.

Using this repoled material, the six transducers mentioned were constructed.[3] Three of the transducers were bonded so that the side of PVF_2 which was charged positive during poling was exposed to the air. (These were labeled the +1, +2, and +3 transducers.) The other three transducers were bonded so that the positive side during poling was epoxied to the brass. (These were labeled the -1, -2, and -3 transducers.)

Two-way reflection mode insertion loss measurements were then performed on all transducers. Insertion loss is defined on the basis of a 50 Ω source generator driving the transmitting transducer and a 50 Ω load connected across the receiving transducer. The results of this experiment are shown in Fig. 3. The graph reveals no significant

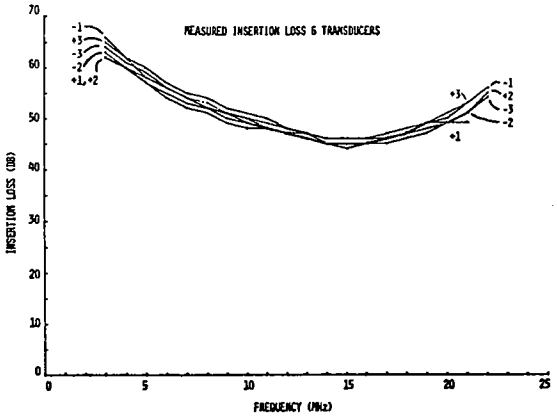

Fig. 3. Measured insertion loss curves for the six text transducers (-1, -2, -3, +1, +2, +3).

differences between the performance of the positive and negative devices. The high degree of similarity between the two sets of curves suggests that the piezoelectric activity of the PVF_2 used in this experiment is spatially symmetric and spatially uniform. Two-way insertion loss measurements were also performed using transducer -1 as the receiver and different transducers as the transmitter. These were consistent with the reflection mode measurements. We conclude that the PVF_2 used in our experiment did have a uniform value of e_{zz} across its thickness.

We next calculated the theoretical insertion loss curve or a transmitting PVF_2 brass-backed transducer using the matrix impedance model. The results were doubled to obtain the two-way insertion loss. The plot of this calculation, along with the average experimental results are shown in Fig. 4.

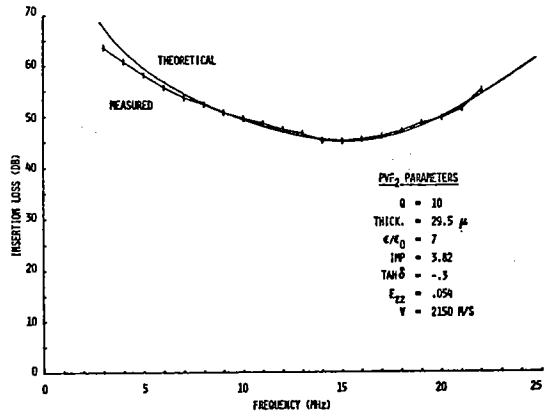

Fig. 4. Average insertion loss of the six test transducers of Fig. 3, and theoretical insertion loss curve adjusted for curve fitting.

By adjusting various parameters used in the calculation we fitted the theoretical curve to the experimental results. Our choice of parameters was guided by previous measurements. A good fit was obtained without drastically changing the original parameter values. This implies that the material properties of PVF_2 are fairly well known and that the experimental and theoretical results are consistent.

The response of PVF_2 to high voltage pulses has also been investigated. The idea behind these experiments was to investigate the maximum nondestructive voltage which can be applied to these transducers and also the linearity of the transducers with respect to voltage. As PVF_2 has relatively low piezoelectric strength compared to ceramic materials, it is of interest to see if this can be compensated by using high input voltages.

The transducers used in this experiment differed from earlier transducers used in that the electrode covering of the PVF_2 was etched back away from the edges of the polymer in order to prevent arcing.

An input voltage pulse was applied to such a transducer immersed in water. The input pulse was triangular in shape with a base width of ~ 200 ns. This pulse generated an essentially bipolar stress wave in the water which was then incident upon another PVF_2 transducer. Figure 5 is a plot of the amplitude of the input signal versus the peak-to-signal observed across the receiving transducer.

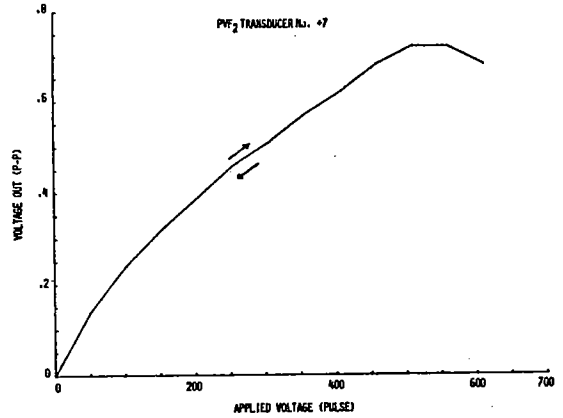

Fig. 5. Measured voltage across receiving transducer versus amplitude of voltage pulse applied to a PVF_2 transducer used as transmitter.

The output voltage is seen to increase in a roughly linear manner up to ~ 600 v(20v/μ). At this point the pulse generator could not supply a larger amplitude output pulse unless the width of the pulse was expanded significantly. This pulse widening resulted in a shift of the pulse energy from high to low frequencies, where the insertion loss is higher. The curve consequently leveled off at this point. Using the same transmitting transducer, the experiment was repeated and was found to yield repeatable results. This shows that PVF_2 transducers can withstand at least 20 v/μ without damage (in a pulse mode), while still operating well. Other experiments of this type suggest that PVF_2 transducers can withstand 45 v/μ without readily apparent damage. In that particular case, however, the transducer did appear to sustain some damage at voltage gradients above 50 v/μ. In either case the upper limit of

applied voltage is significantly larger than the maximum ac voltage which can be applied to most piezoelectric ceramics. For example, the ac depoling field for PZT-5A is ~ .7 v/μ. The above results on linearity are consistent with earlier experiments carried out here. A high power cw rf generator was used to generate high rf voltage at the terminals of a transducer of the above type using 25 μ Kureha film, and the radiated acoustic field strength was monitored with a receiving transducer electrostatically shielded to suppress the direct electrical feedthrough signal. The radiated field strength was accurately linear with applied voltage up to a voltage gradient of 25 v/μ, the highest gradient obtainable from the rf generator. It should be noted that PVF_2 transducers can be excited with high rf electric fields wihtout requiring high terminal voltage by folding and bonding electroded film, producing a multilayer transducer in which voltages of the individual layers are in parallel while their acoustic fields are in series.[4]

The PVF_2 device programs are formally associated with an NSF supported materials program on piezoelectric polymers. Under this program, synthesis of PVF_2 from the monomer is carried out in the Chemical Engineering Department by C. Frank, S. Bowker and students, and PVF_2 film fabrication is carried out in the Center for Materials Research (CMR) by R. Feigelson, R. Route, R. DeMattei and students. Under the present device project we have tested PVF_2 films from this program, by using them to fabricate transducers of the type described above. Figure 6 shows measured two-way insertion

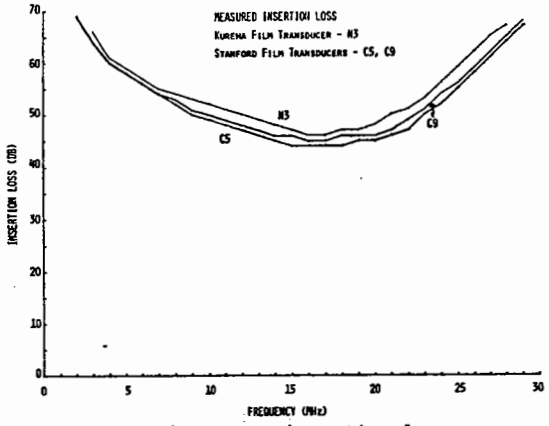

Fig. 6. Measured two-way insertion loss curves for transmitting transducers using Stanford and Kureha films.

loss results on two identical transducers (C5 and C9) made with film (thickness 25 μ) pressed at CMR from commercial polymer powder, compared with that of a transducer (N3) made using Kureha film (thickness 25 μ). In these measurements, the transducer under test was used as transmitter, and a fixed calibrated PVF_2 transducer was used as receiver.

PVF_2 surface wave transducers were used to generate and detect surface acoustic waves on ceramic substrates. Wideband acoustic impulses were easily generated with these assemblies with the dynamic range enhanced by the application of high level input pulses. These transducers were tested on unpolished Si_3N_4 plates containing half penny shaped cracks, to determine their potential for application to nondestructive evaluation. The performance of the transducers was evaluated through measurement of direct and Fourier-transformed reflections from the cracks.[5]

The experimental system is outlined in block diagram form in Fig. 7. A single transducer is

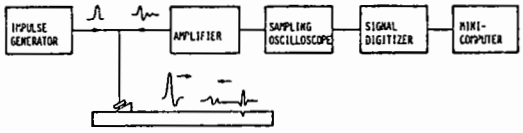

Fig. 7. Block diagram of system employed for surface flaw detection studies.

used as both source and detector. It consists of a 25 micron thick, 1.2 cm square element of uniaxially stretched PVF_2 obtained in sheet form from the Kureha Corporation, already stretched, aluminum coated and poled. The aluminum coatings were removed by etching and replaced with gold on chrome (≈ 1000 Å) evaporated coatings, and the sheets then repoled. The transducer element was attached to a mirror finished brass backing plate with epoxy cement, taking care to obtain a very thin uniform bond. The opposite surface of the backing plate was angled to reduce reflections. It is pivot mounted in a brass holder, as indicated in Fig. 8, with a silicone rubber wedge (RTV 615) placed between the PVF_2 and the ceramic substrate. The orientation of the holder and the angle of the wedge were both adjustable so that the longitudinal-to-surface wave coupling could be optimized.[6]

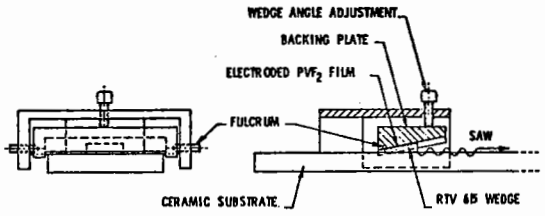

Fig. 8. Sketch of transducer assembly used for surface wave generation and detection.

The PVF_2 transducer was driven by a repetitive monopolar voltage impulse, approximately 300 volts peak amplitude and 50 nanoseconds full width at half amplitude, as indicated in the oscillogram shown in Fig. 9. This led to the launching of a surface wave impulse onto the top surface of the substrate. Surface wave impulses reflected back to this same transducer from the edges of the substrate and from surface flaws led to signals that were easily detected and processed.

As indicated in Fig. 7, the amplified received signal was fed to a sampling oscilloscope that effectively increases the time duration of the submicrosecond received impulses, permitting them to be digitized using a relatively slow analog-to-digital converter.[7] In addition, the sampling oscilloscope also served as a gated amplifier so that any desired temporal portion of the received signal could be selected for viewing and analysis. Hard copy graphs of the various received impulses and their Fourier spectra were obtained in approximately two minutes using a minicomputer and an x-y plotter.

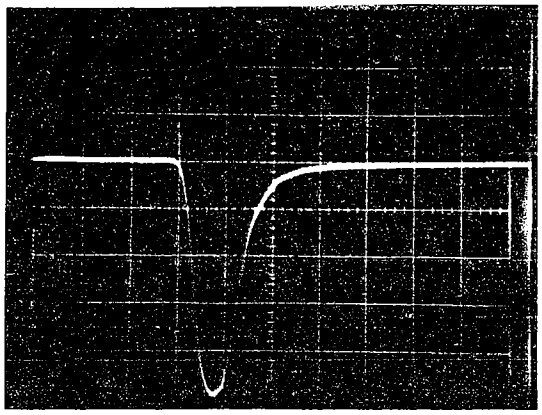

Fig. 9. Oscillogram of voltage impulse employed to excite source transducer. Vertical - 50 V/div. Horizontal - 50 nsec/div.

To indicate the type of data that have been obtained with this system measurements were made using a substrate of 0.64 cm thick, 16 cm x 2.5 cm rectangular silicone nitride Si_3N_4 plate. The top and bottom flat surfaces of the plate were optically polished and the edges were finely ground perpendicular to these surfaces. Three surface flaws were produced adjacent to one end of the plate using the Knoop identation technique.[8] As indicated in the sketch shown in Fig. 10, two flaws designated "Type A," one on the top and the other on the bottom,

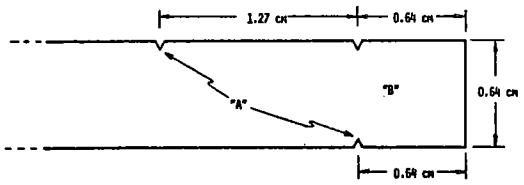

Fig. 10. Schematic diagram indicating flaw locations on ceramic test plate: "Type A" flaws generated with 750 Newton indent load, "Type B" flaw with 500 Newton load.

were produced by applying a 750 Newton force to a diamond indenter; the third "Type B" flaw was generated using a 500 Newton force. This technique yields "half penny" shaped flaws, and these were positioned along, and oriented transverse to, the center line of the flat surfaces, the "Type A" flaws are approximately 900 microns in diameter and the "Type B," 750 microns.

The transducer holder was positioned approximately 1 cm from the opposite end of the substrate and adjusted to maximize the reflection from the top edge. An oscillogram of a portion of the amplified (40 dB) received signal, shown in Fig. 11, contains at succeedingly later times echoes from the two top surface flaws (at 4.2 and 8.6 μsec), the top and bottom end edge echoes (at 10.8 and 13 μsec) and finally the echo from the bottom surface flaw (at 15.2 μsec). The echoes from the three flaws are well above the background noise level; it is to be expected, therefore, that substantially smaller flaws should be detectable even without additional signal processing.

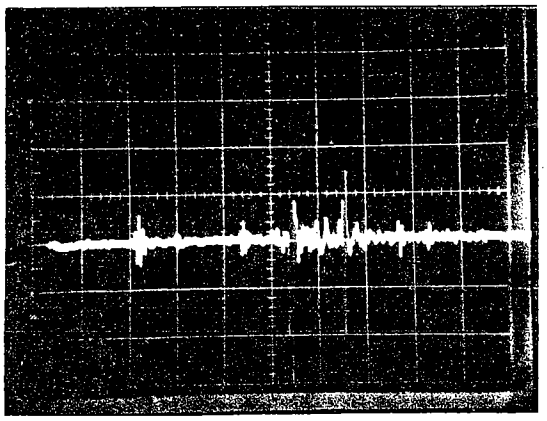

Fig. 11. Oscillogram of amplified (40 dB) received signal indicating echoes from surface flaws at approximately 4.2 μsec, 8.6 μsec and 15.2 μsec, and the edge echoes at 10.8 and 13 μsec. Vertical: 0.5 V/div. Horizontal: 2 μsec/div.

Plots of the portion of the sampled and digitized received signal containing the reflected impulse from the top edge of the plate, and its Fourier spectrum, are shown in Figs. 12(a) and 12 (b), respectively. Note that this impulse is tri-

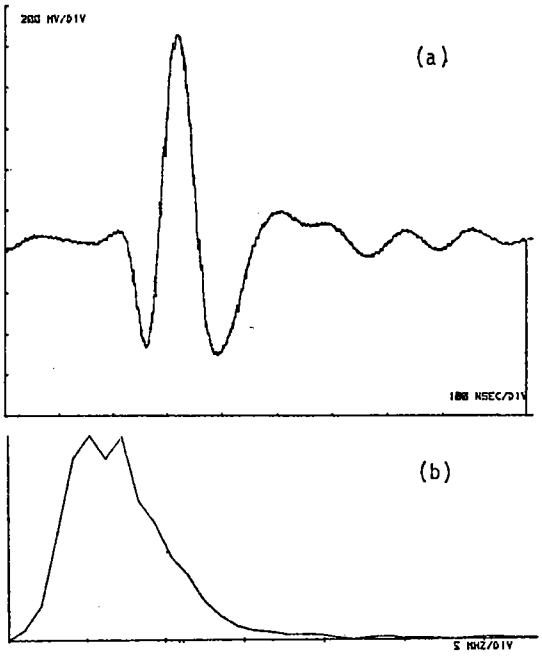

Fig. 12. (a) Plot of received echo from top edge of ceramic plate and (b) its Fourier spectrum.

polar and that it has substantial frequency components over the entire frequency range 0.5 to 10 MHz. This reflected impulse is expected to be reduced to amplitude by approximately 12 dB from the incident impulse.[9] The received signals and corresponding Fourier spectra for the "Type A" and smaller "Type B"

flaw on the top surface of the plate and the "Type A" flaw on the bottom surface are shown in Figs. 13, 14, and 15, respectively. It may be seen that

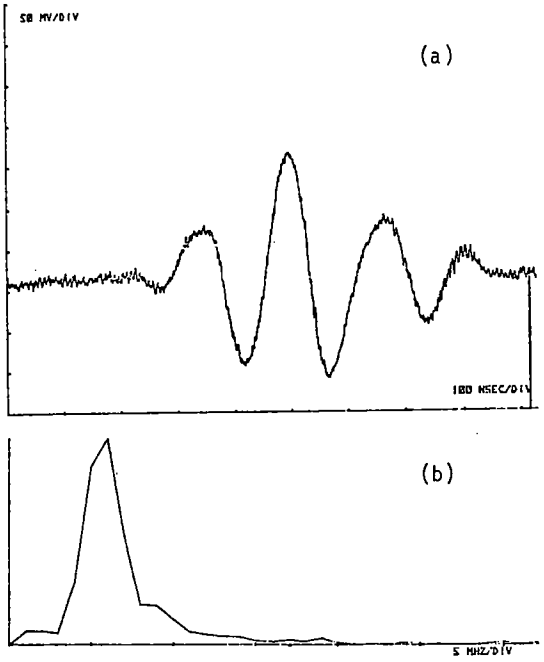

Fig. 13. (a) Plot of received echo from "Type A" flaw on top of plate and (b) its Fourier spectrum.

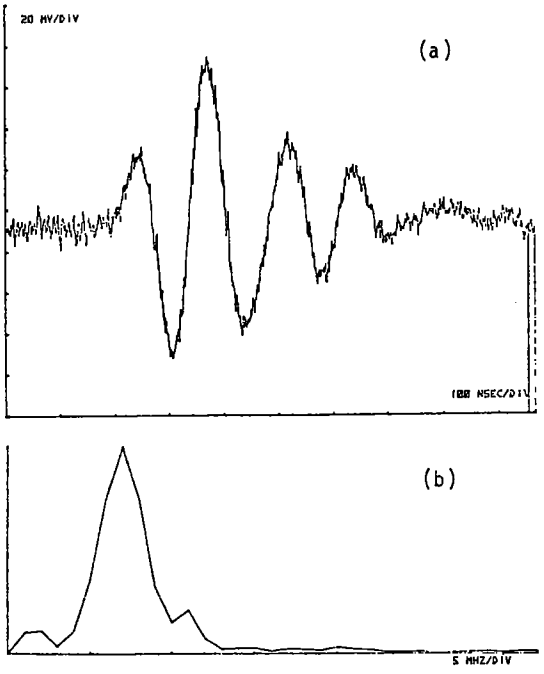

Fig. 14. (a) Plot of received echo from "Type B" flaw on top of plate and (b) its Fourier spectrum.

the peak-to-peak amplitudes for these three impulses are approximately 270, 140 and 170 millivolts, respectively. The latter indicate that flaws on the reverse side of a substrate may be detected. The spectra of the signals from the flaws are substantially different from that of the edge reflection. As expected, both the lower and higher frequencies present in the incident pulse are attenuated in the scattered impulses. The spectrum of the top "Type A" flaw (Fig. 13(b)) peaks at approximately 6 MHz while that of the "Type B" flaw (Fig. 14(b)) peaks at 7 MHz. These correspond closely to the frequencies at which the acoustic wavelength is the same as the length of the flaw. Thus, as expected, the spectra of the scattered signals may yield useful information about the flaw size and other factors.

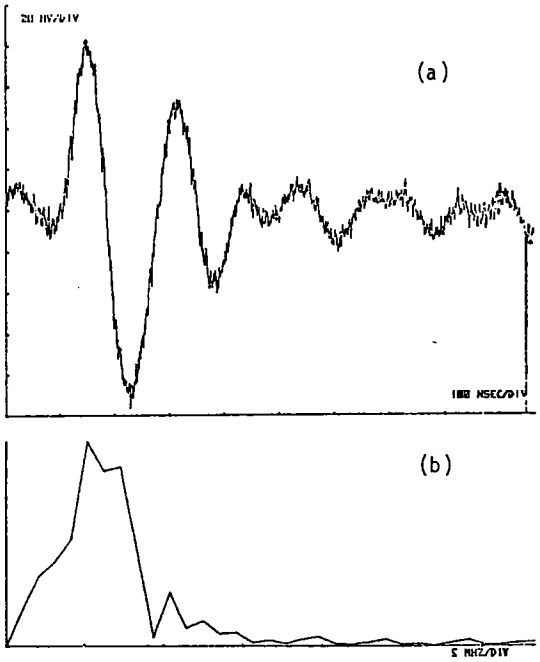

Fig. 15. (a) Plot of received echo from "Type A" flaw on bottom of plate and (b) its Fourier spectrum.

Measurements have also been made on Si_3N_4 plates with fine ground rather than polished surfaces. No substantial increase in the background noise was detected in the frequency range below 15 MHz. This appears to be the upper frequency limit for surface wave generation and detection with the transducer holding and mounting system currently being employed. Impulse propagation studies made in water using the same transducers as sources indicate that when they are driven by voltage impulses of the type shown in Fig. 14, they radiated impulses with spectra extending to 20 MHz and higher. This is illustrated in Fig. 16, where the received impulse and its Fourier spectra are shown for the case of two PVF_2 transducers, brass backed and mounted as described in this paper, one acting as source and the other as detector, used for longitudinal wave studies in water. The electronic and signal processing system is the same as that used in the present study. Note that the received signal spectrum is substantially broader than that shown in Fig. 12. With this result in mind, the design of the holder for the transducer and wedge is being improved in an effort to

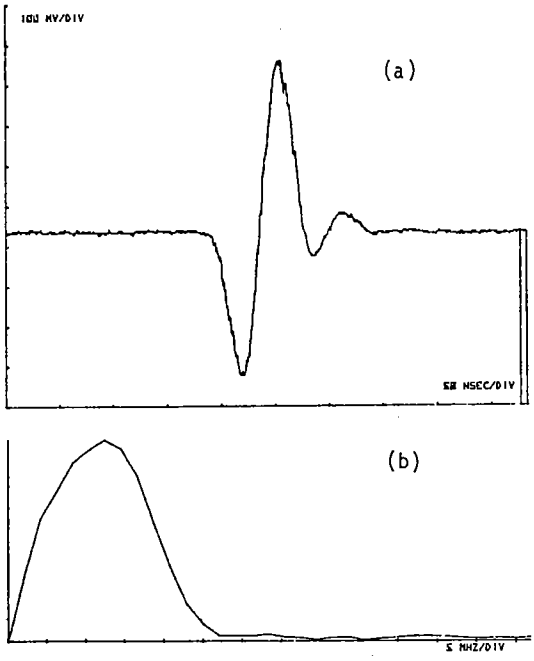

Fig. 16. (a) Plot of received impulse generated and detected in water using two PVF_2 transducers and (b) its Fourier spectrum.

increase the bandwidth and other capabilities of this technique. Further surface wave measurements are in progress on substrates with various smaller sized flaws; these are aimed at obtaining quantitative data on the relationship between flaw signal spectra and flaw length, orientation and depth, to further evaluate the applicability of PVF_2 transducers for such work.

ACKNOWLEDGMENTS

This work was supported by the Office of Naval Research under Contract N00014-77-C-0582, the Air Force Office of Scientific Research under Grant AFOSR-77-3386, and the NSF-MRL Program through the Center for Materials Research at Stanford University under Grant No. DMR77-24222.

REFERENCES

1. S. Hunklinger, H. Sussner, and H. Dransfeld, Festkorperprobleme XVI, p. 267 (1976).

2. L. Bui, H. J. Shaw, and L. T. Zitelli, Electronics Letters 12, 16, 393 (5 August 1976).

3. E. Carome, H. J. Shaw, D. Weinstein, and L. T. Zitelli, "PVF_2 Transducers for NDT," 1979 Ultrasonics Symposium Proceedings.

4. W. H. Chen, H. J. Shaw, D. G. Weinstein, and L. T. Zitelli, "PVF_2 Transducers for NDE," 1978 Ultrasonics Symposium Proceedings, p. 780.

5. E. Carome, K. Fesler, H. J. Shaw, D. Weinstein, and L. T. Zitelli, "PVF_2 Surface Wave Transducers," 1979 Ultrasonics Symposium Proceedings.

6. J. Fraser, B. T. Khuri-Yakub and G. S. Kino, Appl. Phys. Letters 32, 698 (1978).

7. B. T. Khuri-Yakub, private communication.

8. J. J. Petrovic and M. G. Mendiratta, J. Am. Ceram. Soc. 59, 163 (1976).

9. F. Cuozzo, E. L. Cambiaggio, J. Damiano and E. Rivier, IEEE Trans. Sonics and Ultrasonics SU-24, 280 (1977).